Original article

Nuclear Medicine Communications

Impact of point spread function reconstruction on quantitative ^{18}F-FDG-PET/CT imaging parameters and inter-reader reproducibility in solid tumors

Sara Sheikhbahaei[a], Charles Marcus[a], Rick Wray[a], Arman Rahmim[a], Martin A. Lodge[a] and Rathan M. Subramaniam[a,b,c]

Introduction **This study aims to determine the impact of point-spread function (PSF) reconstruction on quantitative PET/computed tomography (CT) indices and the inter-reader reproducibility of these measurements.**

Materials and methods **The study was approved by the Institutional Review Board under a waiver of informed consent. A total of 42 oncology patients with 85 lesions (all ≥ 2 cm) were included. The PET/CT images were reconstructed with PSF (OSEM + TOF, 2i, 21s, all-pass filter) and without PSF (OSEM + TOF, 2i, 21s, 5 mm Gaussian). For each lesion, the maximum, mean, and peak standardized uptake values (SUV), total lesion glycolysis (TLG), and metabolic tumor volume (MTV) were measured by two readers (R1 and R2) using a semiautomatic gradient segmentation method. Intraclass correlation coefficient (ICC) and Bland–Altman analyses were performed.**

Results **There was excellent correlation between non-PSF and PSF reconstruction PET/CT values (ICC ≥ 0.96 for all parameters, $P < 0.0001$). Comparison of PSF with non-PSF images showed a mean bias (percentage change) of + 11.97% (R1) and + 11.94% (R2) for SUV_{max}, + 7.63% (R1) and + 7.82% (R2) for SUV_{mean}, + 7.45% (R1) and + 7.37% (R2) for SUV_{peak}, − 0.82% (R1) and − 0.1% (R2) for TLG, and − 6.68% (R1) and − 5.65% (R2) for MTV. PSF reconstruction resulted in a decrease in MTV in 77.6% (R1) and 83.5% (R2) of lesions. Percentage changes in PSF versus non-PSF indices were not related to the site of the lesions ($P > 0.05$). Close agreement was observed between two readers (ICC ranged between 0.9 and 1.0, $P < 0.0001$).**

Conclusion **The PSF reconstruction increased the SUV_{max}, SUV_{mean}, and SUV_{peak}, as expected, whereas it tended to produce lower values for MTV and had variable effect on TLG. This can be attributed to the ability of PSF reconstruction to better discern tumor uptake from activity spill-out.** ***Nucl Med Commun*** **37:288–296**

Nuclear Medicine Communications 2016, **37**:288–296

Keywords: ^{18}**F-FDG, image processing, oncology, PET, point-spread function reconstruction**

[a]Russell H. Morgan Department of Radiology and Radiological Sciences, [b]Department of Oncology of Johns Hopkins School of Medicine and [c]Department of Health Policy and Management, Johns Hopkins Bloomberg School of Public Health, Baltimore, Maryland, USA

Correspondence to Rathan M. Subramaniam, MD, PhD, MPH, Department of Radiology and Radiology Science, Johns Hopkins Medical Institutions, 601 N. Caroline Street, JHOC 3235, Baltimore, MD 21287, USA
Tel: + 1 410 502 3956; fax: + 1 443 287 2933; e-mail: rsubram4@jhmi.edu

Received 20 August 2015 **Revised** 24 October 2015
Accepted 24 October 2015

Introduction

During the past two decades, fluorine-18 fluorodeoxyglucose PET (^{18}F-FDG-PET) has gained increasing importance in the oncological management of a variety of cancers and has been incorporated in the diagnosis and follow-up surveillance of patients [1–4]. Several studies have consistently reported that ^{18}F-FDG-PET metabolic and volumetric parameters can provide valuable diagnostic and prognostic information that is useful in monitoring the disease course and in therapy response assessment [4–6].

Nevertheless, the spatial resolution of PET imaging is much lower than that of computed tomography (CT) or MRI (< 1 mm), is limited to about 4–6 mm, and is frequently poorer in oncological applications [7,8]. The poor spatial resolution of PET results in undesired cross-contamination between adjacent functional regions with distinct activities, referred to as the partial volume effect. This manifests itself in biased estimation of regional radioactivity concentration [7,9]. Higher system resolution reduces partial volume effects, improving the accuracy of the standardized uptake value (SUV) [7,10]. To improve the qualitative and quantitative accuracy of PET images for a given scanner, various methods for partial volume corrections have been suggested in recent years [7,10–14]. We specify that partial volume correction methods can be adopted after reconstruction or within reconstruction: the latter is commonly referred to as point-spread function (PSF) modeling (also known as resolution modeling) and is more readily available with some clinical scanners.

The introduction and evolution of technological advances such as time of flight (TOF) [15,16] and the implementation of PSF modeling [17,18] within the reconstruction algorithm of PET has been observed to improve the spatial

DOI: 10.1097/MNM.0000000000000445

resolution of images and can impact small, low-intensity lesion detectability [7,8,10,19,20]. Acquisition with TOF can improve coincidence localization and reduce the background noise [21]. Recent studies also suggested that the implementation of PSF reconstruction results in improved as well as more uniform spatial resolution within the field of interest and can increase the image contrast to noise ratios and could potentially decrease the degree of applied postsmoothing filtration compared with conventional PET [11,21,22]. Overall, the improved spatial resolution translates into reduced partial volume effects, improving SUV measurements as seen for phantoms and patients in neurological and oncological studies [18,23]. To date, studies on oncological patients, mostly lung and breast cancer patients, have illustrated that PSF modeling results in a significant increase in the SUV measurement [8, 10,11,23,24]. This suggests that predefined SUV thresholds used for the discrimination of malignant versus benign disease should be interpreted with caution [10].

Recent studies have suggested that volume-based PET/CT parameters, including total lesion glycolysis (TLG) and metabolic tumor volume (MTV), represent the whole tumor activity and may better reflect the overall tumor burden compared with SUV_{max} [25]. Although the impact of PSF reconstruction on SUV has been evaluated in a number of studies [8,10,11,23,24], little is known about its effect on volumetric measurements of PET/CT [8,10]. In addition, inter-reader reliability of ^{18}F-FDG-PET parameters is important for quantitative imaging for therapy response assessment. The inter-reader variability is introduced as readers use semiautomatic software for measurement of quantitative PET parameters in different ways. In this study, we aimed to extend prior studies by evaluating the impact of PSF implementation on the quantitative ^{18}F-FDG-PET/CT indices including MTV and TLG, including inter-reader reliability, in a group of consecutive patients with solid tumors.

Materials and methods

This was a retrospective study performed under a waiver of informed consent and approved by the Institutional Review Board. A total of 42 consecutive patients with different solid tumors including head and neck, breast, lung, and colorectal cancer, who underwent ^{18}F-FDG-PET/CT between April 2014 and June 2014, were included. The ^{18}F-FDG-PET/CT studies were reconstructed both with and without a PSF algorithm.

PET/CT examination and interpretation

The PET scanner used in this study was the Siemens Biograph mCT 128 (Siemens Medical Solutions, Erlangen, Germany). ^{18}F-FDG-PET/CT studies were performed according to routine, institutional clinical protocol. After a minimum of 4–6 h fasting, patients were injected with a standard 5.55 MBq/kg dose of ^{18}F-FDG, to a maximum of 647.5 MBq. Whole-body PET/CT scanning was performed on supine patients with their arms above their head. Helical CT (120 kV; 20–200 mAs; 8.0 noise index) images were obtained with a matrix of 512×512. Beam collimation was 128×0.6 mm, with a pitch of 0.8. Slice increment was 3 mm, and the field of view was 50 cm. The PET portion of the study started ~60 min after ^{18}F-FDG injection, and data were acquired for 3 min per bed position (21 cm axial field of view).

PET images were reconstructed with a three-dimensional ordered-subsets expectation maximization (OSEM) algorithm. PET emission data were corrected for photon attenuation effects using CT images. PET data sets were reconstructed with two algorithms as follows: high-resolution or PSF modeling (OSEM + TOF + PSF, two iterations, 21 subsets, all-pass filter) and conventional modeling without PSF (OSEM + TOF, two iterations, 21 subsets, 5 mm Gaussian). PSF modeling for the mCT involves kernels within the reconstruction algorithm that model both in-plane and cross-plane blurring effects in the projection space, as derived using very careful point source measurements through a 3D positioning robot [26]. The PET/CT studies were interpreted by two readers, one a postdoctoral research fellow (R1) and one a nuclear medicine board-certified physician who is a current PET/CT clinical fellow (R2). The location of each ^{18}F-FDG-avid lesion greater than 2 cm was determined by the readers in advance. Subsequently, the two readers extracted PET/CT quantitative parameters of the PSF and non-PSF reconstruction algorithms, independently for the same lesion. For each lesion, maximum, mean, and peak [5] standardized uptake value (maximum, mean, and peak SUV), TLG, and MTV were measured using a validated gradient segmentation method (PET edge) [27] as implemented by MIM Software Inc. (Cleveland, Ohio, USA). Peak SUV represents automated computed maximal average SUV in a 1.2 cm spherical volume centered in the most metabolically active region within the tumor [5].

Statistical analysis

The absolute changes in PET/CT quantitative parameters (SUV_{max}, SUV_{mean}, SUV_{peak}, TLG, and MTV) after PSF reconstruction, expressing actual units of measurements, were determined as [$PSF_{(value)}$ − non-$PSF_{(value)}$] and shown in the bar plot. The percentage relative changes in each quantitative PET/CT parameter after PSF reconstruction were determined as $[(PSF_{(value)} - \text{non-}PSF_{(value)})/\text{non-}PSF_{(value)}] \times 100$. The relative changes for each ^{18}F-FDG-PET/CT parameter were presented as mean, SD of the difference (precision), and 95% confidence interval (CI). To determine the effect of tumor location and time of scan on the percentage changes in PET parameters between reconstruction algorithms, nonparametric tests (Mann–Whitney *U*, and Kruskal–Wallis *H*) were used. Single-measure intraclass correlation coefficient (ICC) and Cronbach's α statistics were utilized as measures of absolute agreement and

reliability. The ICC ranges between 0 and 1.00, with values closer to 1.00 representing better reproducibility. Values from 0.0 to 0.2 indicated slight, 0.21 to 0.40 indicated fair, 0.41 to 0.60 indicated moderate, 0.61 to 0.80 indicated substantial, and 0.81 to 1.0 indicated almost-perfect reproducibility [28]. Results of the Bland–Altman analysis were also reported for each ^{18}F-FDG-PET/CT parameter. The Bland–Altman scatter plot demonstrates the difference between two reconstruction methods against their mean. The statistical significance level was set at P less than 0.05. Statistical analysis was performed using IBM SPSS Statistics 22.0 (IBM Corp., New York, USA).

Results

A total of 42 consecutive patients with solid tumors were included, whose demographic data are summarized in Table 1. Among these patients, 17 (40.5%) underwent a PET/CT study for initial staging and 25 (59.5%) for restaging of the disease. Overall, a total of 85 lesions including 34 primary tumors, 37 nodal tumors, and 14 metastatic lesions were identified (after excluding the outliers, $n=4$). The mean (SD) number of lesions per patient, all types combined, was 2.02 (1.3).

There were excellent correlations between non-PSF and PSF reconstruction PET/CT values. ICC correlation for all five PET metabolic parameters ranged from 0.96 to 1 ($P<0.0001$), with Cronbach's α values of at least 0.99 (Table 2).

The changes in quantitative PET/CT parameters after PSF reconstruction are illustrated in Fig. 1. Each bar represents the absolute differences for each lesion. Table 3 depicts the mean, SD, and 95% CI of relative changes in quantitative ^{18}F-FDG-PET/CT parameters after PSF reconstruction by each reader.

Comparison of PSF with non-PSF images showed a mean difference (SD) of +11.97 (6.35)% (R1) and +11.94 (6.39)% (R2) for SUV_{max}, +7.63 (6.82)% (R1) and +7.82 (7.01)% (R2) for SUV_{mean}, and +7.45 (5.69)% (R1) and +7.37 (3.39)% (R2) for SUV_{peak}. The 95% limits on agreement for the relative differences in volumetric PET parameters between the techniques were very wide for TLG and MTV, with a mean difference of −0.82 (R1) and −0.11 (R2) for TLG and −6.68 (R1) and −5.65 (R2) for MTV. PSF reconstruction had a variable effect on TLG values and tended to decrease it in 52.9% (45/85, R1) and 48.2% (41/85, R2) of lesions. However, PSF implementation tended to generally produce lower values for MTV and resulted in a decrease in MTV in 77.6% (66/85, R1) and 83.5% (71/85, R2) of lesions. The Bland–Altman plots of differences between two reconstruction methods are shown in Figs 2 and 3.

Table 1 Demographics of the study population

	Mean (SD) or *N* (%)
Age	57.7 (13)
BMI	26.53 (6.13)
BMI ≥ 25	23 (56.1)
Sex	
Male	18 (42.9)
Female	24 (57.1)
Location of primary tumor	
Head and neck	13 (31)
Lung	12 (28.6)
Breast	12 (28.6)
Colorectal	5 (11.9)
Site of lesion	
Primary tumor	34 (40)
Nodal	37 (43.5)
Metastasis	14 (16.5)
Time of PET scan	
Baseline	17 (40.5)
Follow-up	25 (59.5)

Percentage changes in PSF versus non-PSF indices were not significantly associated with the site of primary tumor, location of lesions, and time of scan (staging, follow-up) ($P>0.05$ for all). Bivariate correlation analysis did not show any significant association between BMI and percentage change in PET parameters following PSF reconstruction. The ICC test for absolute agreement between the two readers showed almost-perfect level of consistency (ICC > 0.9 for all parameters). The inter-reader agreement ranged from 0.91 (MTV) to 1 (SUV_{max} and SUV_{peak}) with P values less than 0.0001.

Discussion

Our study showed that the integration of PSF in the reconstruction algorithm of PET produced higher values for SUV_{max}, SUV_{peak}, and SUV_{mean}. Previous studies have consistently shown a similar trend for SUV_{max} [8,23, 29] and SUV_{mean} [8,29]. Hoetjes *et al.* [30] showed that the partial volume correction methods, including PSF reconstruction, could improve the accuracy of SUV without significant decrease in the test–retest variability, and could increase SUV by 5–80% depending on tumor size. Lasnon *et al.* [29] reported that PSF-PET is superior to conventional OSEM-PET in nodal staging of non-small-cell lung cancer and provides considerably higher sensitivity (97 vs. 78%), negative predictive value (92 vs. 52%), and lower negative likelihood ratio (0.04 vs. 0.31) compared with OSEM-PET. The authors suggested that negative PSF-PET would potentially replace pre-operative invasive nodal staging in these patients.

Table 4 summarized a number of studies evaluating the effect of PSF reconstruction on PET parameters [8,10,11, 23,29,31]. According to the EORTC [6] and PERCIST [5] guidelines, relative changes of 25 and 30% for SUV_{max} and SUV_{peak} were considered clinically significant [10]. In a study of 74 lung lesions, Armstrong *et al.* [10] showed that 85% (63/74) and 34% (25/74) of lesions showed greater than 25 and 30% increase in SUV_{max} and SUV_{peak}, respectively, after combined TOF and PSF reconstruction, compared with the OSEM-PET. Although our results showed a significant increase in SUV (max, mean, and peak) after PSF implementation, the mean percentage change is considerably lower than most of the

Table 2 Correlation between PET/CT quantitative parameters with non-PSF and PSF reconstruction

	Non-PSF vs. PSF reconstruction			
	Reader 1		Reader 2	
	Intraclass correlation	Cronbach's α	Intraclass correlation	Cronbach's α
SUV_{max}	0.96 [0.43–0.99]	0.99	0.96 [0.44–0.99]	0.99
SUV_{peak}	0.99 [0.78–1]	1	0.99 [0.76–1]	1
SUV_{mean}	0.97 [0.83–0.99]	1	0.97 [0.81–0.99]	0.99
MTV	0.98 [0.96–0.98]	0.99	0.98 [0.96–0.99]	0.99
TLG	1 [0.99–1]	1	1 [0.99–1]	1

Numbers were rounded to two decimal places.
CT, computed tomography; MTV, metabolic tumor volume; PSF, point-spread function; SUV, standardized uptake value; TLG, total lesion glycolysis.
$P < 0.0001$ in all analyses.

previous reports, and only 1–2% of lesions showed more than 30% change in SUV.

This could be attributed to the fact that in this study we compared images reconstructed without and with PSF in the presence of TOF. Specifically, quantification of SUV is highly dependent on the reconstruction protocol [7,12,32]. Although PSF reconstruction achieves improved spatial resolution compared with non-PSF reconstruction algorithms [10,12,32], previous studies have shown that the utilization of TOF-PET can reduce the propagation of data noise and dramatically improve the image quality [7]. The interaction of PSF and TOF is a curious subject area and one that needs to be further assessed and understood; that is, the absence or presence of TOF can alter how additional incorporation of PSF improves imaging (see Section 5.4 in the study by Rahmim [33]). A recent study compared the changes in SUV measures in different PET reconstructions (OSEM 3D+ TOF vs. OSEM 3D+ TOF+ PSF; matrix size 400×400) in 60 oncological lesions [34]. SUV showed generally higher values using PSF, resulting in SUV ratios (non-PSF/PSF) of less than 1 for all measurements (ratios were 0.84, 0.83, and 0.87 for SUV_{max}, SUV_{mean}, and SUV_{peak}, respectively) [34]. The difference between the reconstruction methods was least for SUV_{peak}, indicating the highest reproducibility of SUV_{peak} [34], which is similar to our reports.

Another possible explanation for the lower percentage changes in our study is that we included only lesions that were larger than 2 cm in size, to minimize the effect of partial volume. A number of studies illustrated a negative correlation between lesion diameters and the degree of increase in SUV after PSF reconstruction [8,10,11], although the results did not always reach statistical significance. Lasnon *et al.* [29] reported that increases in SUV_{max}, SUV_{mean}, and node/background ratio using PSF reconstruction were more marked for lesions smaller than 1 cm compared with larger lesions. Brendle *et al.* [34] also reported that PSF reconstruction leads to a higher degree of SUV overestimation in lesions smaller than 5 ml compared with larger sizes.

In addition, a less marked effect of PSF reconstruction on PET quantification in overweight patients has been suggested by a recent study [29]. Our study did not prove any significant association between BMI and changes in PET quantification following PSF reconstruction.

Recent studies indicated that 'whole-body metabolic burden' or TLG provides important benefits in staging, in tailoring therapeutic strategies, and in outcome prediction of solid tumors [25]. However, volume-based indices were suggested to be influenced by partial volume effect, the segmentation method, and the reconstruction algorithm of the PET scan [12,25]. The actual deviation of volumetric parameters of ^{18}F-FDG-PET, including MTV and TLG, after PSF reconstruction has not been well discussed in the literature. A previous study [10] on patients with lung tumors suggested that the percentage changes in TLG40 (using 40% thresholding of SUV_{max}) following combined TOF and PSF reconstruction were less than 10%, with large variations in the amount of changes [mean (95% CI): −7.5% (−37, +22)]. In addition, a recent phantom study [12] examined the effect of different reconstruction algorithms on quantitative ^{18}F-FDG-PET measurements. The authors showed that, at high contrast, PSF implementation (either PSF+TOF or PSF alone) provided the highest spatial resolution among other algorithms and significantly increased the SUV_{max} by 32%. They also showed that PSF implementation led to considerable reduction (around 9%) in MTV [12]. This reduction may misclassify patients after therapy assessment. The present study is the first, to our knowledge, to examine the dependence of both TLG and MTV on PSF reconstruction. According to our results, there is a large variation in the changes in volumetric PET parameters (MTV and TLG) for PSF reconstruction considering SD as a measure of TLG and MTV variability. However, combined TOF and PSF-PET reconstruction tended to produce lower values for MTV in ~77–84% of lesions compared with TOF-PET.

It is noteworthy that there was almost-perfect correlation between non-PSF and PSF-PET quantification, with ICC correlations of more than 0.95 for all parameters. Further, excellent agreement was observed between two readers in the PET quantification of both reconstruction methods (ICC>0.9 for all parameters). However, the ICC of absolute agreement between two readers is higher for SUV_{max} and SUV_{peak} compared with MTV.

Fig. 1

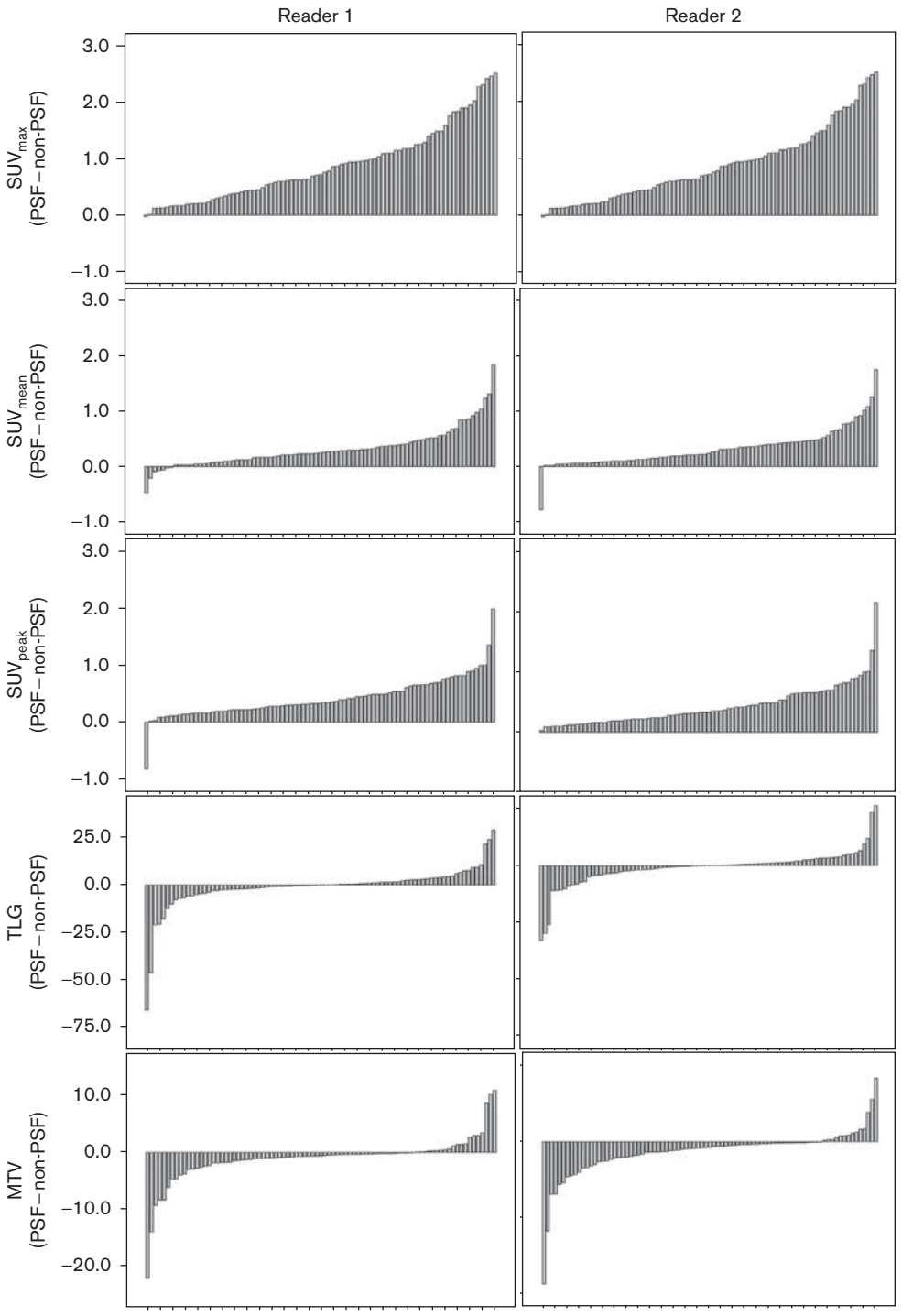

The absolute differences in PET/CT parameters according to the PSF and non-PSF reconstruction for all lesions. CT, computed tomography; MTV, metabolic tumor volume; PSF, point-spread function; SUV, standardized uptake value; TLG, total lesion glycolysis.

Future study should focus on the assessment of the impact of PSF modeling on therapy assessment, as well as the predictive and prognostic value of PET [35], especially as increasing outcome data are being collected. Surprisingly, postreconstruction partial volume correction was found to have no significant effect on prediction of response following treatment in a study involving esophageal cancer [36], and in fact degraded performance in

Table 3 Percentage changes in quantitative PET/CT parameters after PSF reconstruction

	Reader 1			Reader 2		
	Mean	SD	95% CI	Mean	SD	95% CI
Change of SUV_{max} (%)	+11.97	6.35	+3.75 to +25.53	+11.94	6.39	+3.75 to +25.53
Change of SUV_{peak} (%)	+7.45	5.69	+2.79 to +15.89	+7.37	3.39	+3.27 to +14.68
Change of SUV_{mean} (%)	+7.63	6.82	−1.99 to +20.27	+7.82	7.01	+2.79 to +15.89
Change of TLG (%)	−0.82	19.84	−29.50 to +25.67	−0.11	31.32	−42.43 to +16.50
Change of MTV (%)	−6.68	23.52	−38.15 to +35.39	−5.65	41.39	−52.40 to +12.92

Differences were calculated as % (PSF value − non-PSF value)/non-PSF value.
CI, confidence interval; CT, computed tomography; MTV, metabolic tumor volume; PSF, point-spread function; SUV, standardized uptake value; TLG, total lesion glycolysis.

Fig. 2

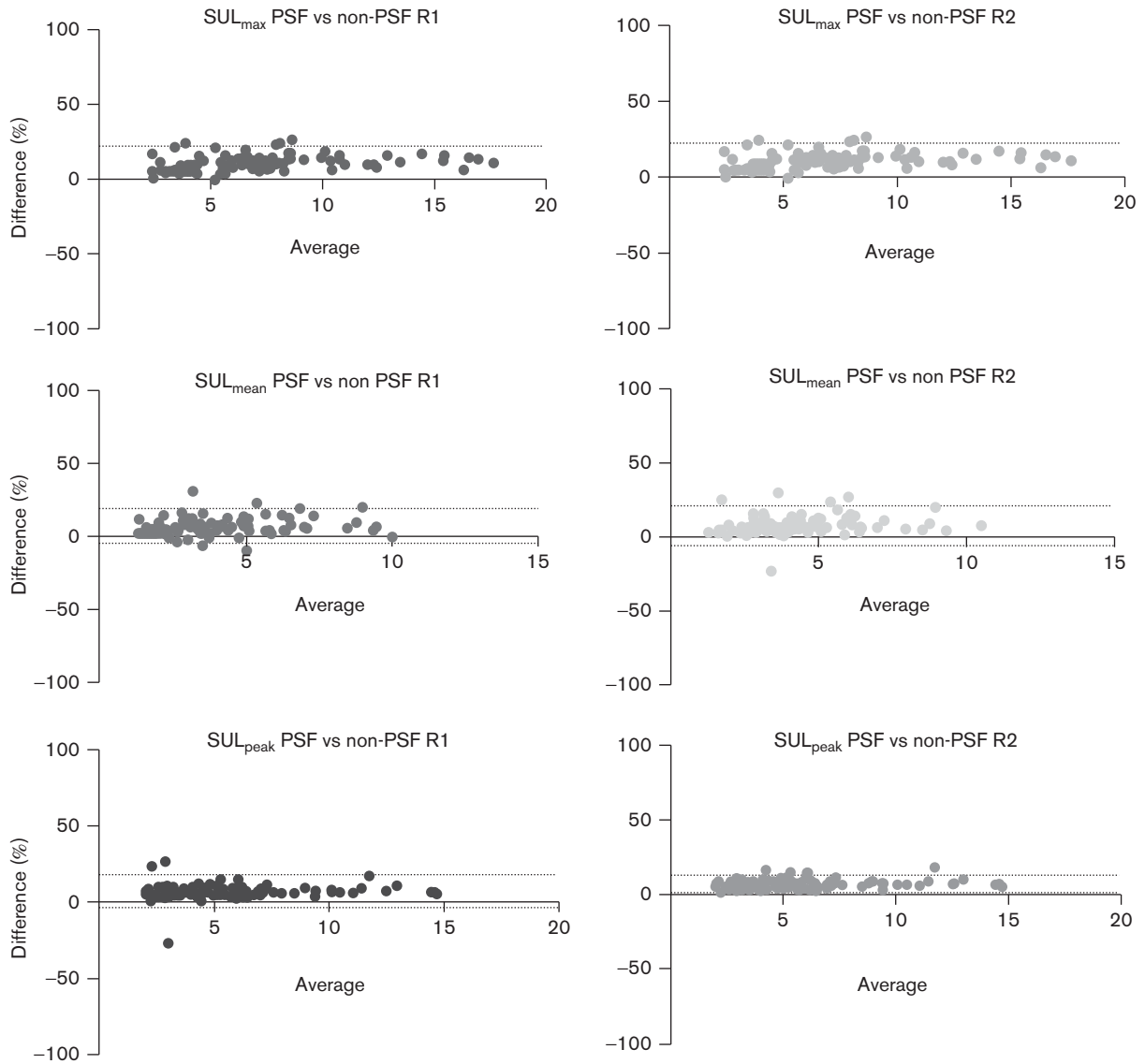

Bland–Altman plot for percentage change in SUV_{max}, SUV_{peak}, and SUV_{mean} for non-PSF and PSF reconstruction between readers 1 and 2. SUL is SUV corrected for lean body mass. PSF, point-spread function; SUV, standardized uptake value.

two other studies (one involving esophageal cancer and another colorectal cancer) [37,38]. This was attributed to the fact that partial volume correction removes the volume information implicit in SUVs, increasing them by greater amounts for complete responders (which are associated with smaller tumors) than for partial nonresponders, resulting in

Fig. 3

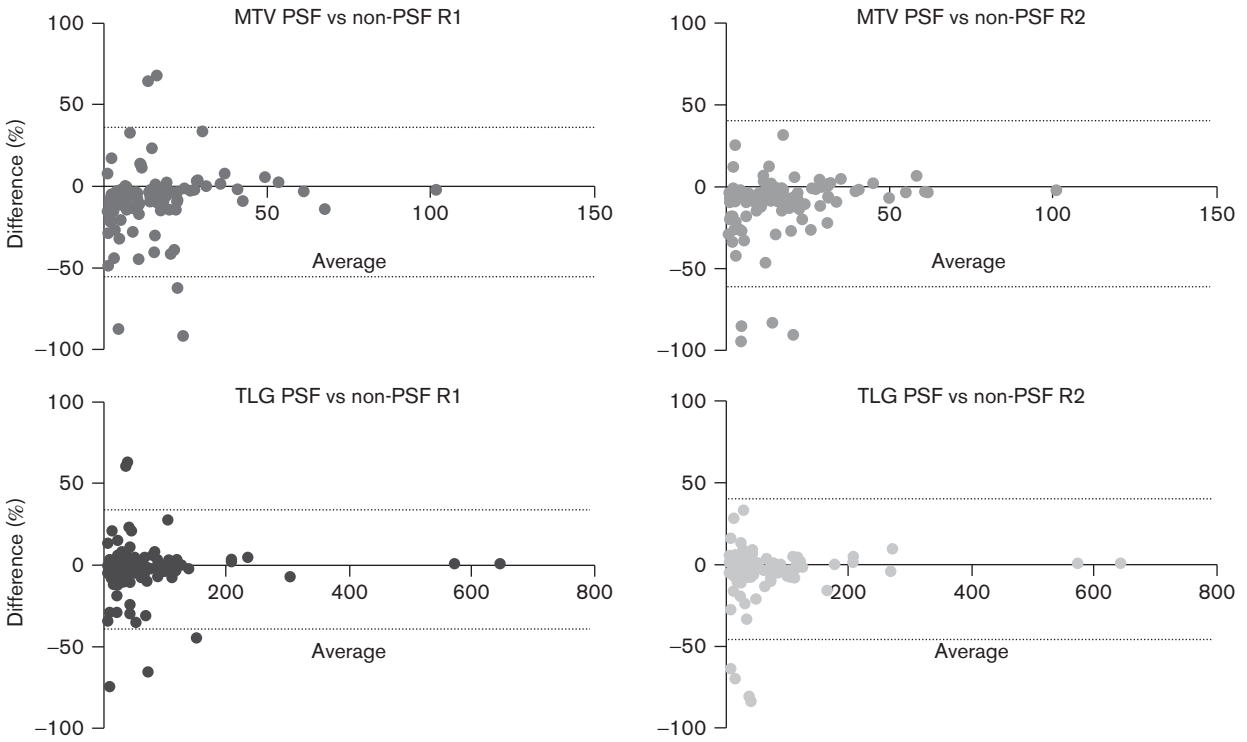

Bland–Altman plot for percentage change in MTV and TLG values for non-PSF and PSF reconstruction between readers 1 and 2. MTV, metabolic tumor volume; PSF, point-spread function; TLG, total lesion glycolysis.

Table 4 Summary of studies evaluating the effect of point-spread function reconstruction on PET quantification

References	Country	Samples	Size restriction	Time of scan	PET reconstruction method	Findings (mean change %)
Akamatsu *et al.* [11]	Japan	41 lymph node metastases in 15 patients	4.6–22.8 mm	–	OSEM + PSF + TOF vs. OSEM	Increase in SUV_{max} (43.3%) Increase in SUV_{mean} (31.6%)
Andersen *et al.* [8]	Denmark	58 lesions in 41 oncological patients	4–44 mm	Staging/ restaging	PSF vs. OSEM	Increase in SUV_{max} (46%) Increase in SUV_{mean} (45%)
Armstrong *et al.* [10]	UK	74 lesions in 68 patients with SPN or NSCL	–	Staging	PSF modeling + TOF vs. OSEM	Increase in SUV_{max} (49%) Increase in SUV_{peak} (27%) Decrease in TLG (7.5%) (NS[a])
Quak *et al.* [31]	France	388 lesions in 23 patients with NHL	–	Restaging	PSF without filter vs. OSEM	Increase in SUV_{max} (54%) Increase in tumor to liver ratio (31%)
Gellee *et al.* [23]	UK	30 patients with lung cancer	–	Staging	PSF vs. OSEM	Increase in SUV_{max} in tumors (35.4%), nodes (42.4%), and metastases (49.4%)
Lasnon *et al.* [29]	France	208 lymph nodes in 46 patients with NSCL	<10 mm or ≥ 10 mm	Staging	PSF vs. OSEM	Increase in SUV_{max} (48%) Increase in SUV_{mean} (28%) Increase in node-background ratio (27%)

NHL, non-Hodgkin lymphoma; NS, not significant; NSCL, non-small-cell lung cancer; OSEM, ordered subsets expectation maximization; PSF, point-spread function; SPN, solitary pulmonary nodule; SUV, standardized uptake value; TOF, time of flight.
[a]Correction was made for recovery effect and motion blur.

diminished intergroup differences. It is very plausible for PSF modeling to produce a similar detrimental effect on the discrimination power. However, the key point to be made is that this is not a shortcoming of PSF modeling, but rather of existing methods that rely solely on SUV uptake to predict outcome. By contrast, multimetric combined assessment may result in enhanced clinical task performance (e.g. dual metric SUV and volume) [39], and it is plausible in this more sophisticated framework that partial volume correction in general, and PSF modeling specifically, can further improve clinical tasks.

Our study has some limitations, including lack of lesion/background uptake comparisons and use of lesions

restricted to larger than 2 cm. We restricted this study to minimize the effect of partial volume on our assessment of PSF versus non-PSF reconstruction. Our sample population included a heterogeneous sample of oncological patients. However, this reflects day-to-day clinical practice and real-world assessment, which is important for PSF implementation in clinical practice. In the present study, 5-mm Gaussian smoothing was used in the non-PSF algorithm but no additional smoothing was used in PSF reconstruction. Thus, there is a mismatch of post-filtering between PSF and non-PSF reconstruction, and quantitative differences are expected due to both PSF reconstruction and the difference in smoothing. The image reconstruction and the degree of smoothing in this study accurately reflect our clinical practice. These factors should be considered while comparing our results with other centers. The intention behind the PSF images was to produce a high-resolution image that may be useful for visual assessment, with the understanding that the quantitative SUV data will not be directly comparable to the conventional (non-PSF) images.

Conclusion

PSF reconstruction produced higher values for SUV_{max}, SUV_{mean}, and SUV_{peak}. It tends to produce lower values for MTV and has variable effect on TLG. The reconstruction method of ^{18}F-FDG-PET/CT should be considered in reporting quantitative parameters, in subsequent lesion classification, and in comparing studies for therapy assessment.

Acknowledgements

Conflicts of interest

Dr Subramaniam is a consultant for GE Healthcare and has received research grants from Bayer HealthCare. For the remaining authors there are no conflicts of interest.

References

1 Delbeke D. Oncological applications of FDG PET imaging: brain tumors, colorectal cancer, lymphoma and melanoma. *J Nucl Med* 1999; **40**:591–603.
2 Agarwal A, Marcus C, Xiao J, Nene P, Kachnic LA, Subramaniam RM. FDG PET/CT in the management of colorectal and anal cancers. *Am J Roentgenol* 2014; **203**:1109–1119.
3 Humbert O, Cochet A, Coudert B, Berriolo-Riedinger A, Kanoun S, Brunotte F, Fumoleau P. Role of positron emission tomography for the monitoring of response to therapy in breast cancer. *Oncologist* 2015; **20**:94–104.
4 Sheikhbahaei S, Marcus C, Subramaniam RM. ^{18}F FDG PET/CT and head and neck cancer. *PET Clin* 2015; **10**:125–145.
5 Wahl RL, Jacene H, Kasamon Y, Lodge MA. From RECIST to PERCIST: evolving considerations for PET response criteria in solid tumors. *J Nucl Med* 2009; **50** (Suppl 1):122S–150S.
6 Young H, Baum R, Cremerius U, Herholz K, Hoekstra O, Lammertsma AA, *et al.* Measurement of clinical and subclinical tumour response using [^{18}F]-fluorodeoxyglucose and positron emission tomography: review and 1999 EORTC recommendations. European Organization for Research and Treatment of Cancer (EORTC) PET Study Group. *Eur J Cancer* 1999; **35**:1773–1782.
7 Bettinardi V, Castiglioni I, De Bernardi E. PET quantification: strategies for partial volume correction. *Clin Transl Imaging* 2014; **2**:199–218.
8 Andersen FL, Klausen TL, Loft A, Beyer T, Holm S. Clinical evaluation of PET image reconstruction using a spatial resolution model. *Eur J Radiol* 2013; **82**:862–869.
9 Soret M, Bacharach SL, Buvat I. Partial-volume effect in PET tumor imaging. *J Nucl Med* 2007; **48**:932–945.
10 Armstrong IS, Kelly MD, Williams HA, Matthews JC. Impact of point spread function modelling and time of flight on FDG uptake measurements in lung lesions using alternative filtering strategies. *EJNMMI Phys* 2014; **1**:99.
11 Akamatsu G, Mitsumoto K, Taniguchi T, Tsutsui Y, Baba S, Sasaki M. Influences of point-spread function and time-of-flight reconstructions on standardized uptake value of lymph node metastases in FDG-PET. *Eur J Radiol* 2014; **83**:226–230.
12 Rogasch JM, Hofheinz F, Lougovski A, Furth C, Ruf J, Großer OS, *et al.* The influence of different signal-to-background ratios on spatial resolution and F18-FDG-PET quantification using point spread function and time-of-flight reconstruction. *EJNMMI Phys* 2014; **1**:12.
13 Erlandsson K, Buvat I, Pretorius PH, Thomas BA, Hutton BF. A review of partial volume correction techniques for emission tomography and their applications in neurology, cardiology and oncology. *Phys Med Biol* 2012; **57**:R119–R159.
14 Rousset OG, Rahmim A, Alavi A, Zaidi H. Partial volume correction strategies in PET. *PET Clin* 2007; **2**:235–249.
15 Moses WW. Recent advances and future advances in time-of-flight PET. *Nucl Instrum Methods Phys Res A* 2007; **580**:919–924.
16 Karp JS, Surti S, Daube-Witherspoon ME, Muehllehner G. Benefit of time-of-flight in PET: experimental and clinical results. *J Nucl Med* 2008; **49**:462–470.
17 Rahmim A, Qi J, Sossi V. Resolution modeling in PET imaging: theory, practice, benefits, and pitfalls. *Med Phys* 2013; **40**:064301.
18 Schaefferkoetter J, Casey M, Townsend D, El Fakhri G. Clinical impact of time-of-flight and point response modeling in PET reconstructions: a lesion detection study. *Phys Med Biol* 2013; **58**:1465–1478.
19 Kadrmas DJ, Casey ME, Conti M, Jakoby BW, Lois C, Townsend DW. Impact of time-of-flight on PET tumor detection. *J Nucl Med* 2009; **50**:1315–1323.
20 Kadrmas DJ, Casey ME, Black NF, Hamill JJ, Panin VY, Conti M. Experimental comparison of lesion detectability for four fully-3D PET reconstruction schemes. *IEEE Trans Med Imaging* 2009; **28**:523–534.
21 Conti M. Focus on time-of-flight PET: the benefits of improved time resolution. *Eur J Nucl Med Mol Imaging* 2011; **38**:1147–1157.
22 Tong S, Alessio AM, Kinahan PE. Noise and signal properties in PSF-based fully 3D PET image reconstruction: an experimental evaluation. *Phys Med Biol* 2010; **55**:1453–1473.
23 Gellee S, Page J, Sanghera B, Payoux P, Wagner T. Impact of the point spread function on maximum standardized uptake value measurements in patients with pulmonary cancer. *World J Nucl Med* 2014; **13**:128–131.
24 Apostolova I, Wiemker R, Paulus T, Kabus S, Dreilich T, van den Hoff J, *et al.* Combined correction of recovery effect and motion blur for SUV quantification of solitary pulmonary nodules in FDG PET/CT. *Eur Radiol* 2010; **20**:1868–1877.
25 Carlier T, Bailly C. State-of-the-art and recent advances in quantification for therapeutic follow-up in oncology using PET. *Front Med (Lausanne)* 2015; **2**:18.
26 Panin VY, Kehren F, Michel C, Casey M. Fully 3-D PET reconstruction with system matrix derived from point source measurements. *IEEE Trans Med Imaging* 2006; **25**:907–921.
27 Werner-Wasik M, Nelson AD, Choi W, Arai Y, Faulhaber PF, Kang P, *et al.* What is the best way to contour lung tumors on PET scans? Multiobserver validation of a gradient-based method using a NSCLC digital PET phantom. *Int J Radiat Oncol Biol Phys* 2012; **82**:1164–1171.
28 Landis JR, Koch GG. The measurement of observer agreement for categorical data. *Biometrics* 1977; **33**:159–174.
29 Lasnon C, Hicks RJ, Beauregard JM, Milner A, Paciencia M, Guizard AV, *et al.* Impact of point spread function reconstruction on thoracic lymph node staging with 18F-FDG PET/CT in non-small cell lung cancer. *Clin Nucl Med* 2012; **37**:971–976.
30 Hoetjes NJ, van Velden FH, Hoekstra OS, Hoekstra CJ, Krak NC, Lammertsma AA, Boellaard R. Partial volume correction strategies for quantitative FDG PET in oncology. *Eur J Nucl Med Mol Imaging* 2010; **37**:1679–1687.
31 Quak E, Hovhannisyan N, Lasnon C, Fruchart C, Vilque JP, Musafiri D, Aide N. The importance of harmonizing interim positron emission tomography in non-Hodgkin lymphoma: focus on the Deauville criteria. *Haematologica* 2014; **99**:e84–e85.
32 Prieto E, Domínguez-Prado I, García-Velloso MJ, Peñuelas I, Richter JÁ, Martí-Climent JM. Impact of time-of-flight and point-spread-function in SUV quantification for oncological PET. *Clin Nucl Med* 2013; **38**:103–109.
33 Rahmim A, Tang J. Noise propagation in resolution modeled PET imaging and its impact on detectability. *Phys Med Biol* 2013; **58**:6945–6968.

34 Brendle C, Kupferschläger J, Nikolaou K, la Fougère C, Gatidis S, Pfannenberg C. Is the standard uptake value (SUV) appropriate for quantification in clinical PET imaging? Variability induced by different SUV measurements and varying reconstruction methods. *Eur J Radiol* 2015; **84**:158–162.

35 Alessio AM, Rahmim A, Orton CG. Point/counterpoint. Resolution modeling enhances PET imaging. *Med Phys* 2013; **40**:120601.

36 van Heijl M, Omloo JM, van Berge Henegouwen MI, van Lanschot JJ, Sloof GW, Boellaard R. Influence of ROI definition, partial volume correction and SUV normalization on SUV-survival correlation in oesophageal cancer. *Nucl Med Commun* 2010; **31**:652–658.

37 Hatt M, Le Pogam A, Visvikis D, Pradier O, Cheze Le Rest C. Impact of partial-volume effect correction on the predictive and prognostic value of baseline ^{18}F-FDG PET images in esophageal cancer. *J Nucl Med* 2012; **53**:12–20.

38 Maisonobe JA, Garcia CA, Necib H, Vanderlinden B, Hendlisz A, Flamen P, Buvat I. Comparison of PET metabolic indices for the early assessment of tumour response in metastatic colorectal cancer patients treated by polychemotherapy. *Eur J Nucl Med Mol Imaging* 2013; **40**:166–174.

39 Tylski P, Dusart M, Necib H, Vanderlinden B, Buvat I. Which parameter should be considered to characterize tumor changes in patient monitoring using FDG-PET? *J Nucl Med* 2008; **49**:382P.